Full Length Research Paper

The spraying field characteristics and distribution of deposition of droplets of electrostatic oiler

Zhao-Hui Wang*, Fa-Ping Wang, Jia-Rong Fan, Quan-Jie Gao and Jia-Qing Wang

College of Mechanical Automation, Wuhan University of Science and Technology, Wuhan, Hubei, 430081, China.

Electrostatic oiler are made as the research object, the multiple field spray characteristics of air flow field, electric field and discrete fog field in the process of spraying were analyzed. The influence of electrostatic spray deposition characteristics has been studied by changing the electrostatic voltage and electrode gap. The experiment about electrostatic oil spray has been verified. The results show that droplets of axial velocity are larger in the outlet of spray field near the larger intensity area. Near the metal plate, the air flow accelerates the droplets and makes the fog area diffused. Due to the droplets deposition and diffusion on the metal plate, the air is around in motion. With the electrostatic voltage increases, the droplet size decreases to a certain value then basically unchanged and afterwards the droplet size increases as the electrodes distance increases. The droplet deposition area increases first and then decreases with the increase in voltage, and then decreases with the increasing in electrodes distance; the density fluctuation of the droplet deposition is uniform and the deposition amount is moderate. When the voltage reaches 50 to 60 kV and the electrode spacing reaches 195 to 225 mm, the electrostatic spray atomization effect is better.

Key words: Electrostatic spraying, electrostatic oiler, multi-field characteristics, droplet deposition distribution, spraying experiment.

INTRODUCTION

Atomization effect of the liquid medium has very important influence on the electrostatic spray performance. Compared with other surface deposition technique, electrostatic spraying makes droplet distribution is more uniform. The deposition amount on the target object, the uniformity and adsorption are significantly improved (Wang et al., 2012; Xie et al., 2000). Electrostatic spraying not only can save coating and reduce the degree of pollution, but also make the

spraying process mechanized, continuous and reduce scrap. It can obtain excellent coating properties and improve labor productivity greatly (Wang et al., 2011). Electrostatic spraying multi-field characteristics and distribution of droplet deposition affect the atomization of the liquid medium directly; it is a new topic which must be studied in the current engineering and natural sciences intersection field. It has a value in important theoretical significance and application in promoting energy saving

and low-carbon economy.

Electrostatic spraying is implemented in air flow field, electric field and discrete fog field. It involves electrostatics, plasma, fluid mechanics and other knowledge fusion. Chen and Zhao, (2010) discussed the influence of the distribution characteristics of electric field to the charged droplets effect in the electric liquid two phase flow field. It indicated that the quality of the charged droplets and the distribution characteristics of electric field are closely related. Ye et al. (2002) simulated the electrostatic coating process with electric-air coupled. He calculated the size distribution of particles, and obtained the charge distribution of particles through experiments. Gu et al. (2010) achieved the stable jet cone jet mode, and analyzed the characteristics of flow field, electric field and fog field, but the analysis of coupled three field and spray effect is not deep enough.

Currently the fragmentation mechanism study of charged spray droplets is more, but relatively few studies on the droplet spray deposition characteristics. Colbert and Cairncross (2005) established the mathematical model of electric field, continuous of the flow field and particle trajectories in electrostatic spray. He simulated and obtained the spray particle distribution characteristics, and analyzed the main factors of affecting the coating thickness distribution. Jung et al. (2010) by changing the voltage between the nozzle and the substrate, the distance between the nozzle and the substrate, and the moving speed of the nozzle, studied the particles spraying process and deposition characteristics in the multi-nozzle device. Zohdi (2013) analyzed the impact and deposition process of the charged particle on the charged substrate, by changing electric field intensity gradually on the substrate. Sun et al. (2012) analyzed the effect of the gas stream on spray drift in three-dimensional space, and studied the effect of different wind speed and spray height on droplets distribution trend and deposition amount. He established a prediction model of droplet deposition amount and deposition rates which is based on this method. Wang et al. (2013) made the air curtain and air-force auxiliary spray system as the research object, analyzed the droplet deposition distribution of the charged spray and the uncharged spray under the different wind speed. Ru et al. (2014) established the settlement movement of droplets and adhesion force model using three-dimensional coordinate system, and analyzed droplet distribution and charged droplet effect on adhesion characteristics under electrostatic spraying or non-static effects of spray. However, above studies do not consider the effect of electrostatic spray coating deposition properties by changing the applied voltage and the distance between the electrodes, limiting the widespread use of electrostatic spraying.

Based on the research, the electrostatic oiler can be made as the research object. The writers studied the multi-field spray characteristic of the air flow field, electric field and discrete fog field and other fields in electrostatic spraying process. Then the influence of charged droplet deposition characteristics was analyzed by changing electrostatic voltage and electrode gap. Finally related spray effects of electrostatic oiler have been verified by experiment. In this paper, the calculated and experimental results will provide theoretical and scientific basis for the precision control of electrostatic spraying.

Spray performance

Electrostatic spraying working principle

The working principle of the electrostatic oiler spraying is shown in Figure 1. When the blade of electrostatic oiler connects with the negative high voltage DC power, the high-voltage electrostatic field formed between the blade and the steel plate. Since the blade edge is relatively sharp and the radius of curvature is so small that the point of the blade generates the corona discharge phenomenon. In this case, the air molecules are ionized into positive and negative ions. These ions can move rapidly along the electric-power line, and the positive ions are neutralized toward the oil injector blade. The negative ions are accelerated and fly to the field plate bringing the positively charged. During this time, the negative ions collide with oil droplets and make the oil droplets charged. With the increasing negative charge on the droplet surface, the electrostatic repulsion between the electric charges will be increased. The droplets will be broken when the electrostatic repulsion exceeds the surface tension of the droplets. Thus, it is the atomization phenomenon. Finally, the atomization oil droplets will be sprayed onto the plate uniformly.

Electrostatic spraying multi-field coupling process

The multi-field of electrostatic spray atomization process includes the air flow field, space fog field and the electric field, which is the mutual coupling of the three field. The multi-field coupling relationship diagram of the electrostatic spraying is shown in Figure 2. The electric field affects the flow field by the wind power, and affects the field fog droplets by the electrostatic force. The flow field acts on the droplet spray field by the aerodynamic drag force, and has momentum exchange with fog field. The fog field affects the electric field distribution through the space-charge, and acts on the flow field through gas two-phase coupling.

Multi-field solver coupling calculation

To establish the multi-field coupling model of the electrostatic spraying, the electrostatic field be customized
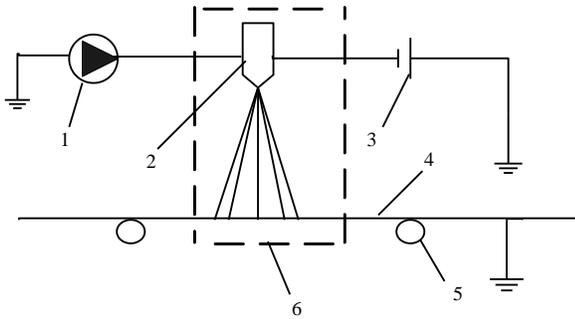
Figure 1. Working principle of electrostatic oiler. 1, Oil supply system; 2, blade; 3, high voltage power supply; 4, steel plate; 5, roller; 6, oil room.
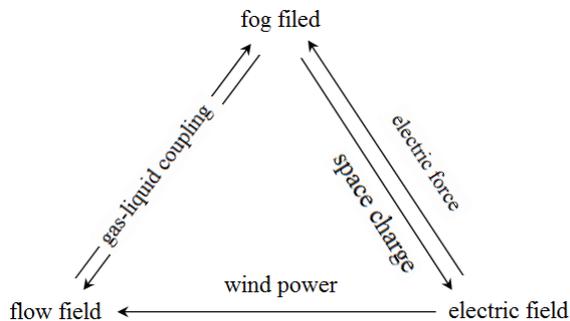

Figure 2. Multi-field coupling of the electrostatic spraying.

in the form of the scalar field, then it added to the spray model. The effect on the liquid is written into Navier-Stokes (N-S) equation in the form of electric force. The electrostatic field distribution can be simplified based on the specific model. The coupled electrostatic field specific process follows: Firstly the electric field distribution can be calculated and the velocity field can be solved. Thereby position of the free surface can be determined. Redistributed the quantities of two-phase and the accurate potential distribution can be solved. After that, we calculate the N-S equation on the basis of the potential distribution, and the results can be fed back to the electric field calculation formula to recalculate the potential distribution of the changed flow field and then a cycle will be completed.

Spraying droplet deposition characteristics

Particle size distribution: The particle size distribution formed by the electrostatic spraying depends on the operating voltage, the electrode spacing and the physical properties of the liquid and other factors. It is an important parameter to judge the quality of electrostatic spraying. In the process of liquid atomization broken into

tiny droplets, the liquid surface tension will inhibit the cracking and deformation of the droplets, and make the droplets become spherical. The most intuitionistic diameter for the description of the spherical droplet size parameter is the diameter; the description of the non-spherical droplet size adopts the equivalent diameter.

Effective deposition area

Electrostatic spraying expects droplets cover larger deposition area after the spraying transport process. The droplet deposition area is related with the liquid pressure, flow rate, operating voltage and other parameters. However, due to the different density of the droplet deposition regions, the deposition density is more uniform and larger in central area, but the periphery is very uneven sporadic deposition. In the calculations, the scattered region is regarded as noneffective region. In the central region, the deposition density of the region is larger and more uniform and it becomes effective region.

Deposition density

The size of the effective deposition area only can display the size of the deposition range and it cannot represent the uniformity of deposition. The droplet deposition density is able to show the uniformity of the droplet deposition distribution. When the liquid is injected from the nozzle to reach the different deposition locations, the number of droplet deposition at each position is different. The deposition density is an important assessment parameter to representation the uniformity of the droplet distribution in the deposition area.

Model

Based on the schematics of electrostatic oiler spraying, the oil room model of electrostatic oiler can be shown in Figure 3. In order to calculate the multi-field and spray deposition characteristics, the simulation model of oil room is established. The length and width of the model are both 40 mm, and the height is 275 mm. The nozzle length is 20 mm; the diameter of nozzle is 2 mm (Wang et al., 2011). Hypermesh software is used for meshing the three-dimensional model of the electrostatic spraying. Totally, there are 1694050 units and 1750680 nodes. The droplet particles are tracked in the calculation process, until it collides with the surface. During this time, depending on the different impact velocity of the droplet particles, the droplet particles adhere to the target surface or rebound eventually. In the electrostatic spray process, if the electrode spacing are too small, the liquid will not fully atomize. If the electrode spacing are too large, the electric field intensity will decrease quickly, and the droplets will not be fully charged and cannot be
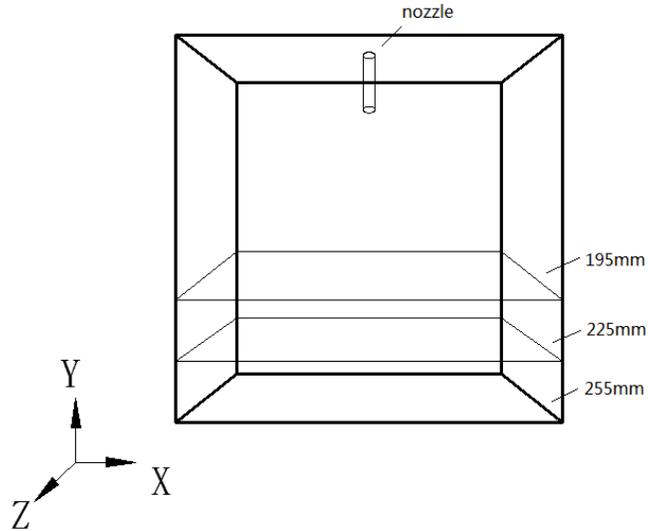
Figure 3. The oil room model of electrostatic oiler.

Table 1. Dielectric characteristics for electrostatic spraying.

Material	Temperature (°C)	Viscosity (mm^2/s)	Surface tension (N/m)	Conductivity (s/m)
Anti-rust oil	45	11.8	0.025	3

atomized. Therefore, in order to study the effects of the electrode spacing on the deposition characteristics, according to the experimental conditions at the normal operating range of the electrostatic oiler spray, we select the electrode spacing at 195, 225 and 255 mm for analysis.

We assume that the charged droplets are spherical, and all the droplet particles are produced near the nozzle. The droplet particles distribute along the X and Z axes randomly. The multi-field simulation of the electrostatic spraying process belongs to the multi-phase flow problem. The finite element solver of the FLUENT software is used for solving the transport equation of the continuous phase and discrete phase model in lagrangian coordinate. Since the energy of the droplet particles is much greater than the kinetic energy of random temperature, so the droplet particles' Brownian motion are ignored (Doyle et al., 1964). In the electrostatic spraying process, the specific calculation parameters are set as follows:

1. Discrete phase injection source parameters: The material used is the rust oil, its dielectric characteristics are shown in Table 1. The nozzle fluid flow is 0.05 ml/s, the electrostatic spraying operating voltage range is 30 to 70 kV, and the rest of the steel plate boundary potentials are zero. Above all is set as the working condition of electrostatic spraying.

2. The boundary conditions parameters: We use UDF procedure to customize the source term introduction of electric force; the spraying port is set as the inlet to provide the liquid. The liquid inlet is a circular cross-section of spherical particles and it is generated by a random order. The discrete phase boundary surface conditions of computational area can be set as the liquid film. The other import, export and discrete phase boundary wall will be set as the escape particles. The material inside calculation area is air. Taylor analogy crushing model and evaporation model can be used, and the collision restitution coefficient can be set to 0.8, then the phase coupling calculation is performed until the final calculation iterative is convergence.

3. Simulation parameters: Eulerian-Lagrangian coupling algorithm can be used, so the gas continuous phase and the droplets dispersed phase around the spray droplets can be calculated. The gravity of spray particles is considered to exist in the calculation.

Calculation and analysis

Multi-field electrostatic spraying characteristics

Air flow field: The longitudinal cross-sectional axial airflow velocity contours in the electrostatic spraying computational domain are shown in Figure 4 when the voltage is 50 kV. The axial flow velocity is larger near the
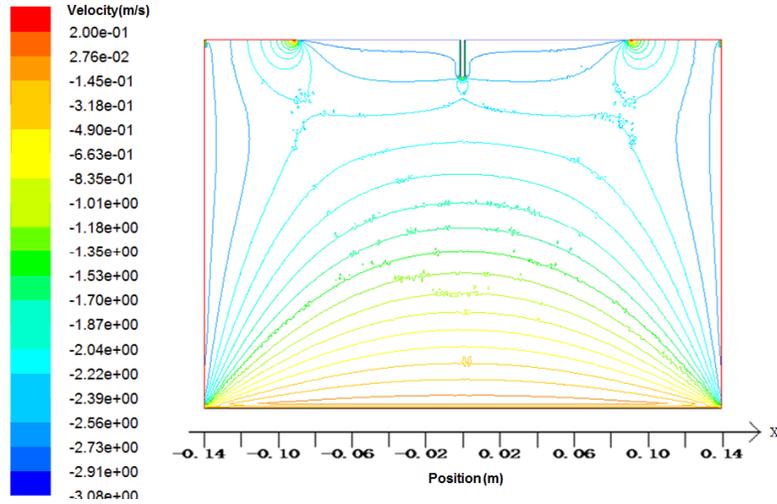
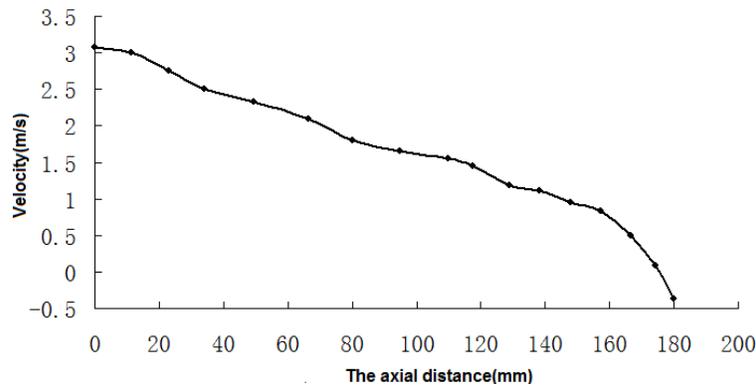**Figure 4.** Axial flow velocity contours.

Figure 5. Axial flow velocity variation.

central axis of the nozzle, because the high speed of the droplets is near the nozzle. Therefore the air is accelerated, and the axial air flow velocity can reach the maximum at 3.08 m/s. When it close to the metal plate, the axial air flow velocity drops dramatically, and be blocked from the plate and the direction of the axial flow is changed. Figure 5 is the axial air flow velocity variation, with the increasing axial distance, the air flow velocity is decreasing, ultimately approach zero.

Spatial Electric field: The electric field we studied does not calculate the effect of the charged ions in the air, nor the electric field of charged droplets formed itself, it is just the spatial electric field distribution by the given potential. The potential distribution in longitudinal section is shown Figure 6a, within 20 mm from the nozzle to the plate, the equipotential lines are very dense and the electric field strength is large. Within this range, the electric field force

is large, the droplets accelerate process is significantly. Outside the scope of 20 mm, the electrical potential line distribution is sparse, the electric field strength decreases rapidly along the axial and the radial directions, then the effect of the electric field force on the droplets becomes smaller and smaller. Figure 6b shows a longitudinal sectional view on the radial distribution of the field intensity. The radial field strength near the nozzle is large. More closer to the metal plate in place, smaller the radial field intensity. Because of getting larger electric force, the droplets are accelerating break up into small droplets and the abruption speed also increases to a certain extent.

Figure 7 shows a radial field strength variation. The radial field strength is over a wide range near the nozzle. In this range the electrostatic force is large. The velocity rapidly increases along the direction of the field lines. Because the electric field affecting the droplets decreases, the field strength decreases rapidly along the radial.
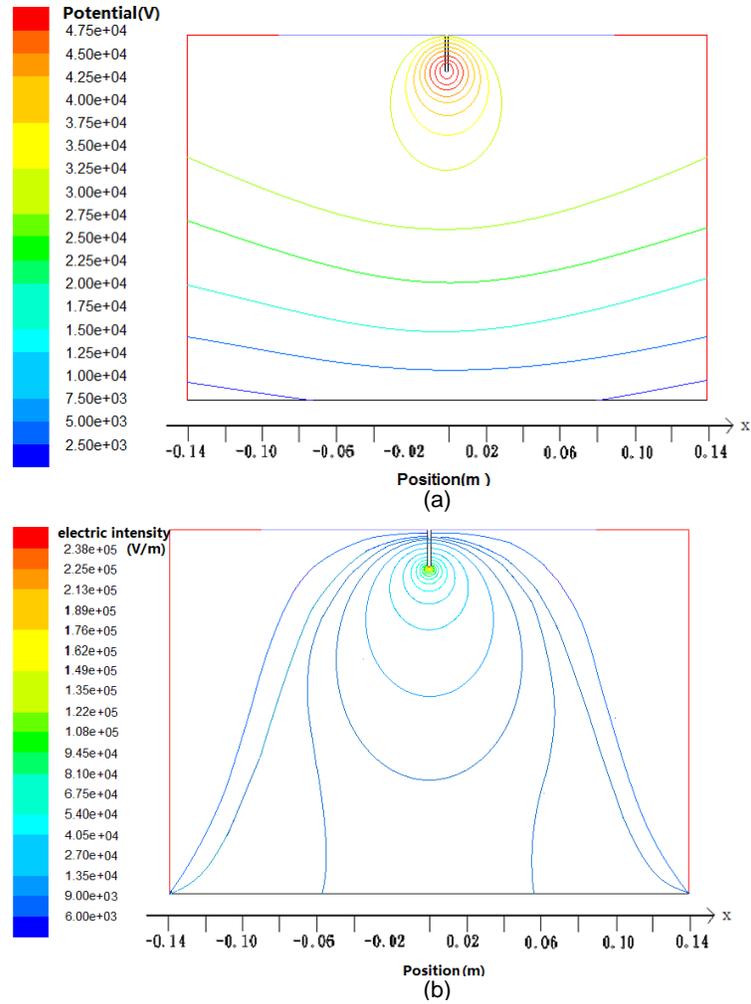
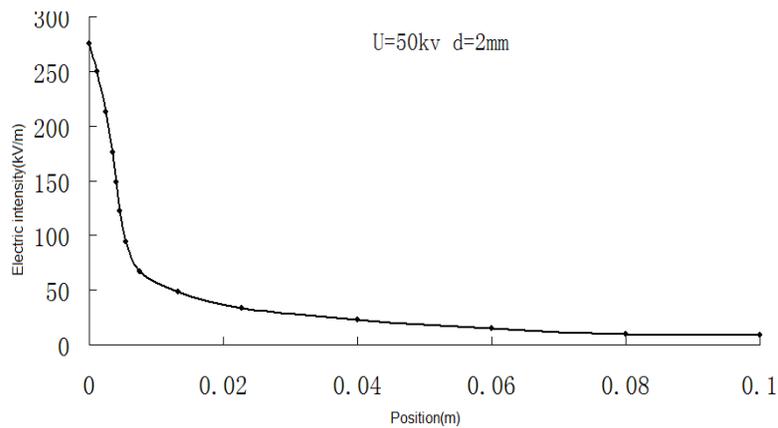**Figure 6.** Electric field distribution; a, potential; b, radial field intensity.

Figure 7. Radial field strength variations.

Discrete fog field

Figure 8 shows a discrete phase fog spatial distribution, it

has been calculated after 0.07 s at the voltage of 50 kV, and the droplet is deposited on the metal plate at the moment. To study the droplet velocity distribution on the
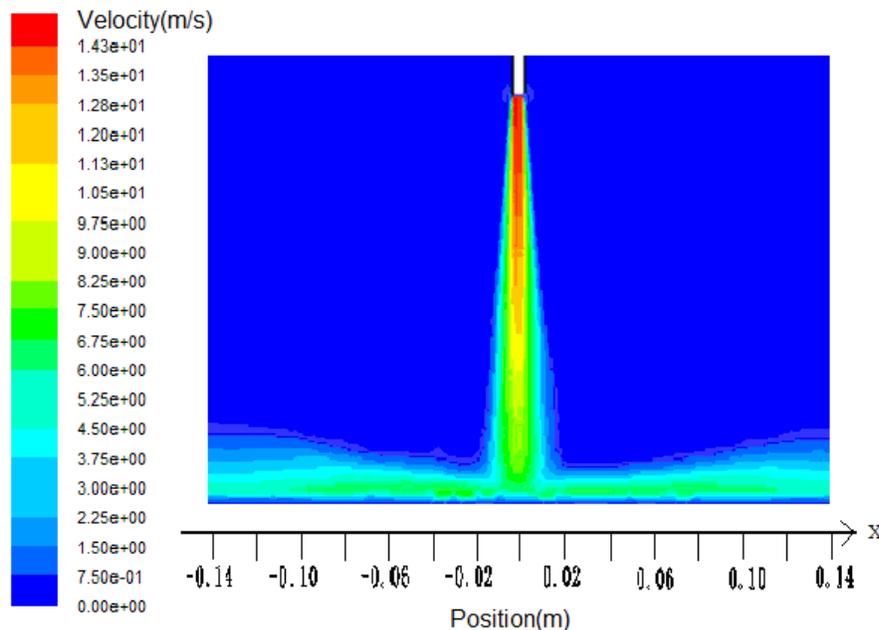
Figure 8. Fog spatial distribution.

cross-section of different distance away from the nozzle, we select, respectively three sections to study the distribution about the radial and axial droplet velocity along the radial direction. The distances of sections from nozzle are 54, 108 and 162 mm.

The axial and radial velocity distributions of the droplet are shown in Figure 9. As can be seen from Figure 9a, the axial velocity of the droplet increases near the nozzle, and the axial velocity of the droplets at the edge is smaller than the center. As can be seen from Figure 9b, the spray droplets have the maximum value of the radial velocity near the central axis. The droplet velocity increases significantly near the metal plate, that is because of the peripheral airflow near the metal plate, So that the droplet accelerates along the radial.

Electrostatic spraying droplet deposition

Discrete phase droplet deposition amount: Figure 10 shows the electrostatic spraying effects when the distance between electrodes is 195 mm. The oil spraying is cone-shaped between the voltage of 30 to 50 kV, and the oil spray tapered angle is larger, but the droplet distribution is very uneven. When the voltage exceeds 50 kV, the spray angle decreases, but the droplet distribution becomes uniform gradually. When the operating voltage achieves 60 kV, the spray angle almost unchanged and the droplet is distributed evenly, at the moment the electrostatic spraying achieves a better effect.

In the specific boundary parameters, the height of the electrostatic spraying are 195, 225 and 255 mm, and the

operating voltage is varying within a range of 30 to 60 kV. The charged droplet deposited clouds are shown in Figure 11. We can directly found the rough droplet diameter and effective deposition area of the electrostatic spraying deposited on the substrate.

Droplet size distribution

When computing iterative convergence, by capturing electrostatic spraying droplet particles in different locations, we get the droplets diameter amount distribution. Figure 12 is the discrete amount probability density function of droplet size histogram under different electrode spacing. When the operating voltage is 30 kV, the range of the peak diamter of number of probability density function is 90 to 120 μm, and the electrostatic voltage is low at this time. The droplets is not completely smashed to achieve the equilibrium state, its size distribution does not show a normal regular shape. When the operating voltage exceeds 40 kV, the droplets are nearly completely broken, the atomizing effect is better than before. The discrete probability density function of droplet size shows the shape of a normal distribution, which is consistent with the practical application. The peak droplet size of the probability density function corresponding to the droplet diameter is reduced from the range 80-110 to 70-100 μm. It shows that with the operating voltage increasing, the droplet diameter decreases effectively.

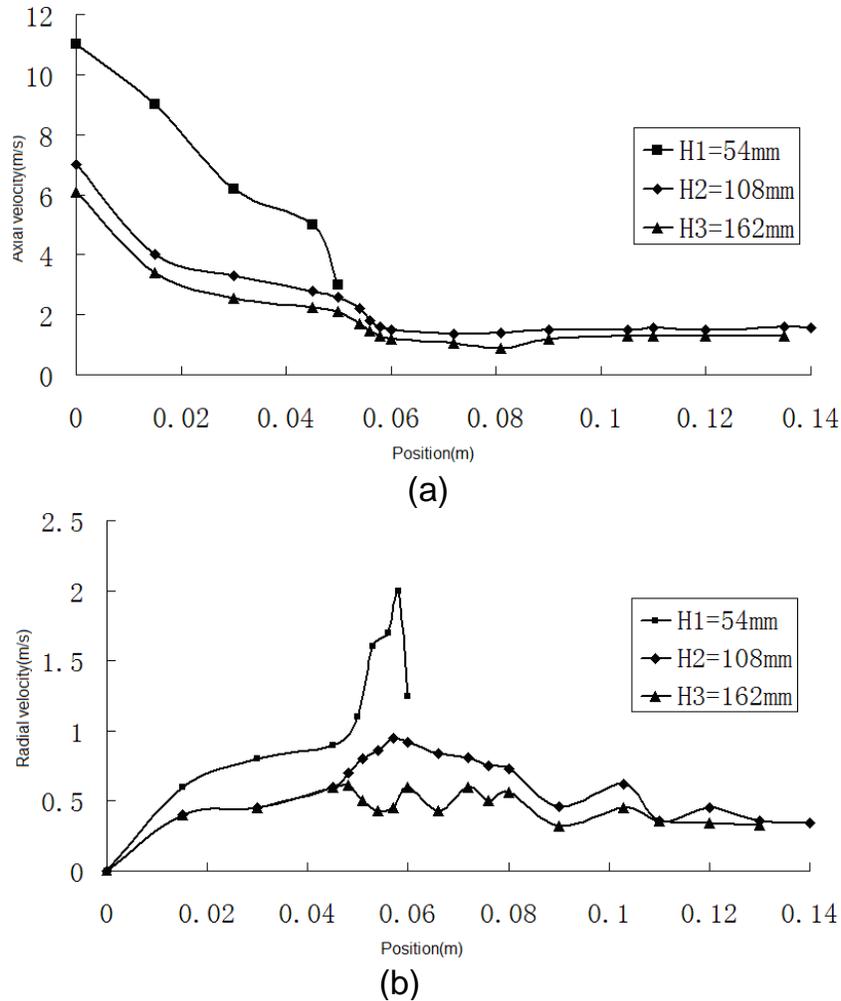With the distance between electrodes decreasing, the number of probability density functions of the droplet size

(a)

(b)

Figure 9. Droplet velocity distribution; (a) axial velocity; (b) radial velocity.
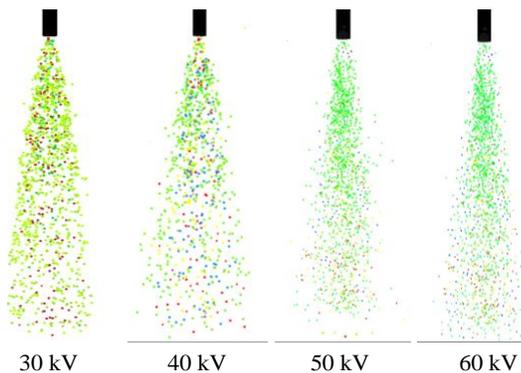

Figure 10. Electrostatic spraying effect when the distance between electrodes is 195 mm.

distribution through the smallest diameter of the droplet number density increases from 0.5 to 0.75. Since the electrode spacing decreasing leads to the electric field

strength increase, it is easy to make the large-diameter droplets be broken into small droplets. At the electrode spacing of 225 and 255 mm, the probability density function shape of the droplet diameter is very consistent. It indicates the droplet broken has reached the basic equilibrium at the distance away from the nozzle outlet of 225 mm. Reducing the distance between spacing electrodes will not significantly reduce the droplet size distribution interval, but the droplet size distribution interval keeps significantly decreasing trend.

Effective deposition area

Figure 13 shows the effective drops deposited area under different electrode spacing and the operating voltage. Since the spray cone angle is decreasing with the electrode spacing increasing, but the jet length is constant when the voltage is over 30 kV. When the voltage keeps a certain value, with the increase of the
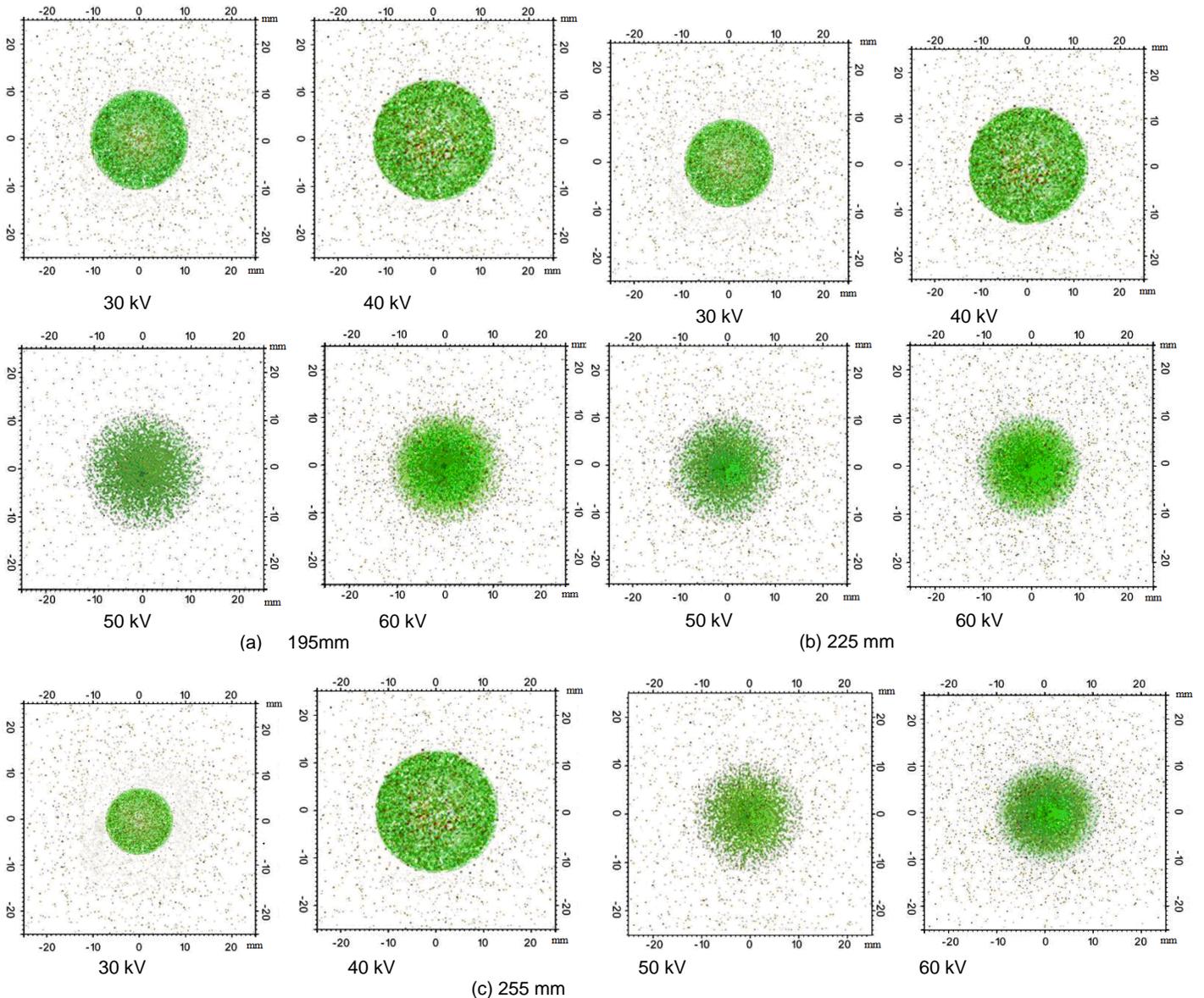
Figure 11. Amount of electrostatic spray deposition under different operating voltages and electrode spacing.

distance between the electrodes, the effective droplet deposited is decreased. Firstly, under the effect of electrostatic force, the droplets diffuse along the field lines in all directions, but not only limited to radial and axial diffusion. Secondly, due to the electrostatic induction, in addition to the part of molecules in the liquid jet core area, the majority of fog drops molecules with the same electrical charge. Since the charge same-sex repulsion, the charged droplets will be diffused toward all directions. Based on this, when the voltage is 30 to 40 kV, the effective droplet deposition area increases significantly. When the voltage between 40 and 50 kV and the electrode spacing is 195 mm, the effective droplet deposition area achieve the maximum 615 mm^2.

When the voltage is around 60 kV, the effective deposited area is decreased. It has the direct relationship with the reduction of the spray angle. When the voltage is further increased to 70 kV, because the jet length substantially zero and the spray angle is further reduced, so the effective deposited area is also followed by a sharp decrease.

Deposition density

Figure 14 shows the droplet deposition distribution under the different working voltage and the electrode spacing, it shows the variation trend of the deposited droplet on the
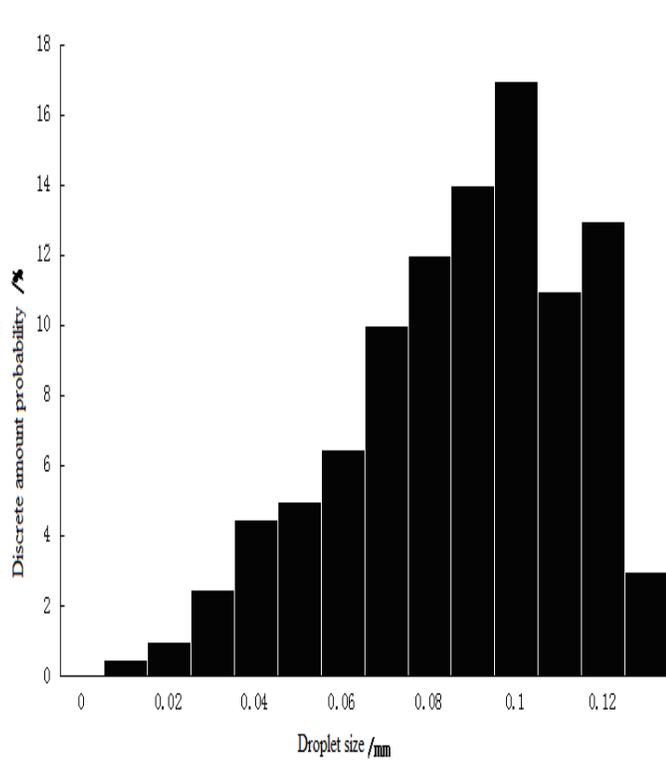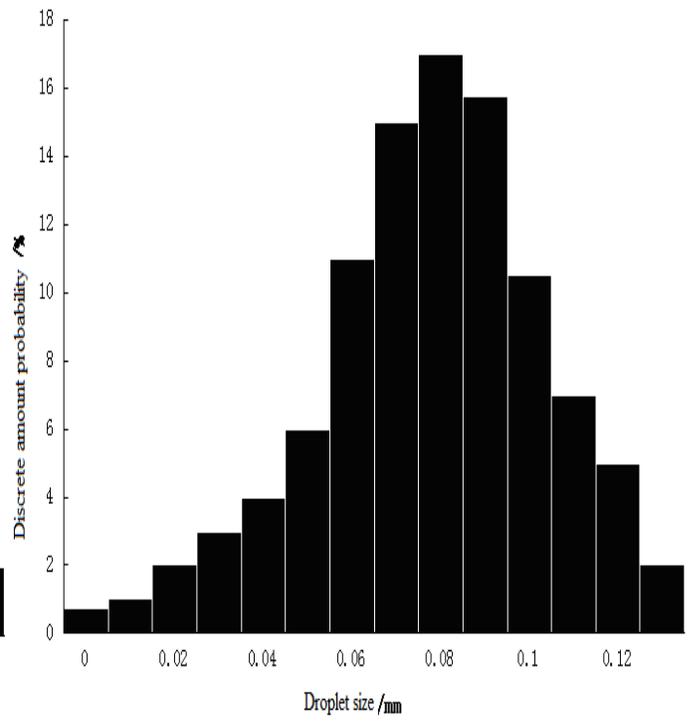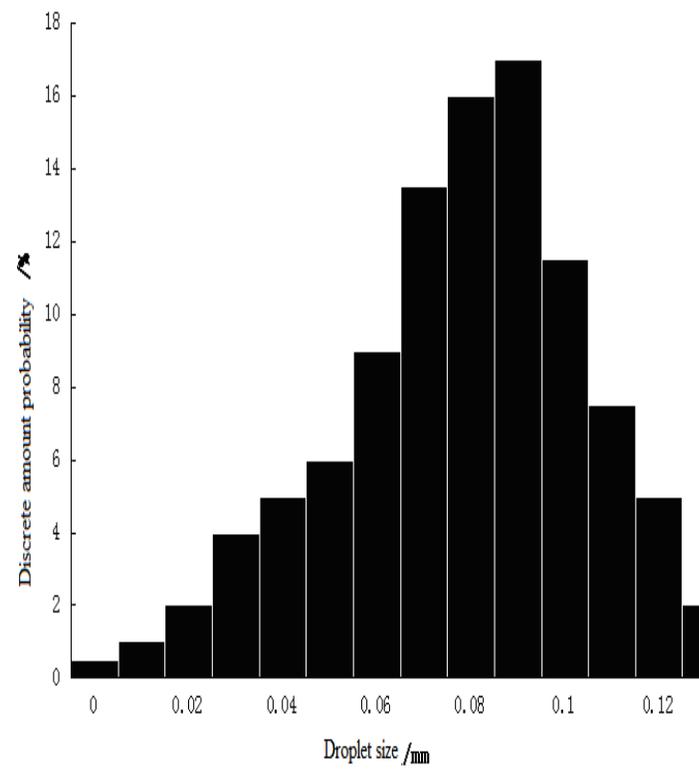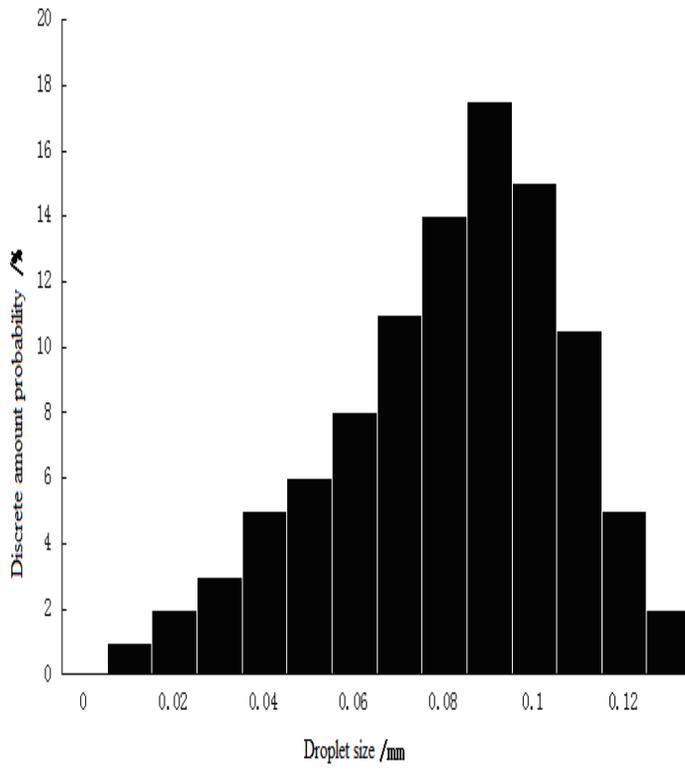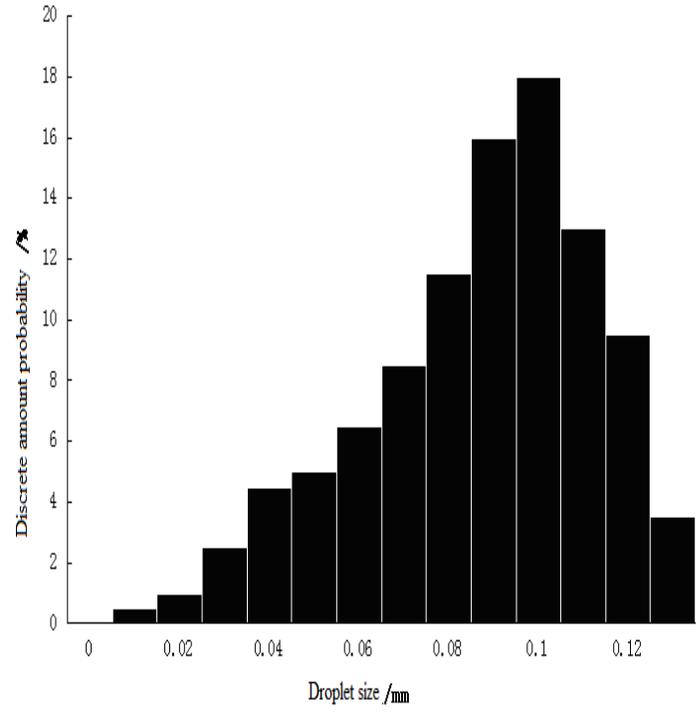
30kV

40kV

50kV

60kV

(a)   195mm
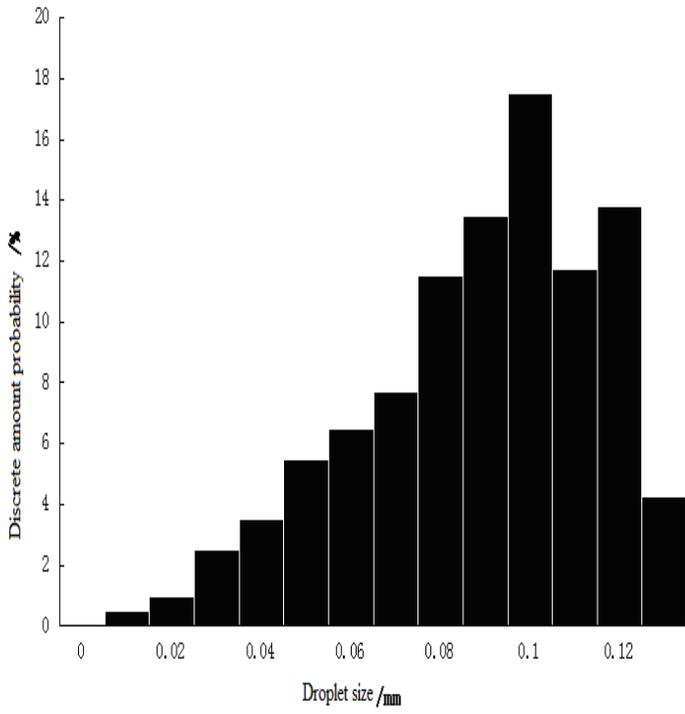
30kV

40kV

50kV

60kV

(b) 225mm
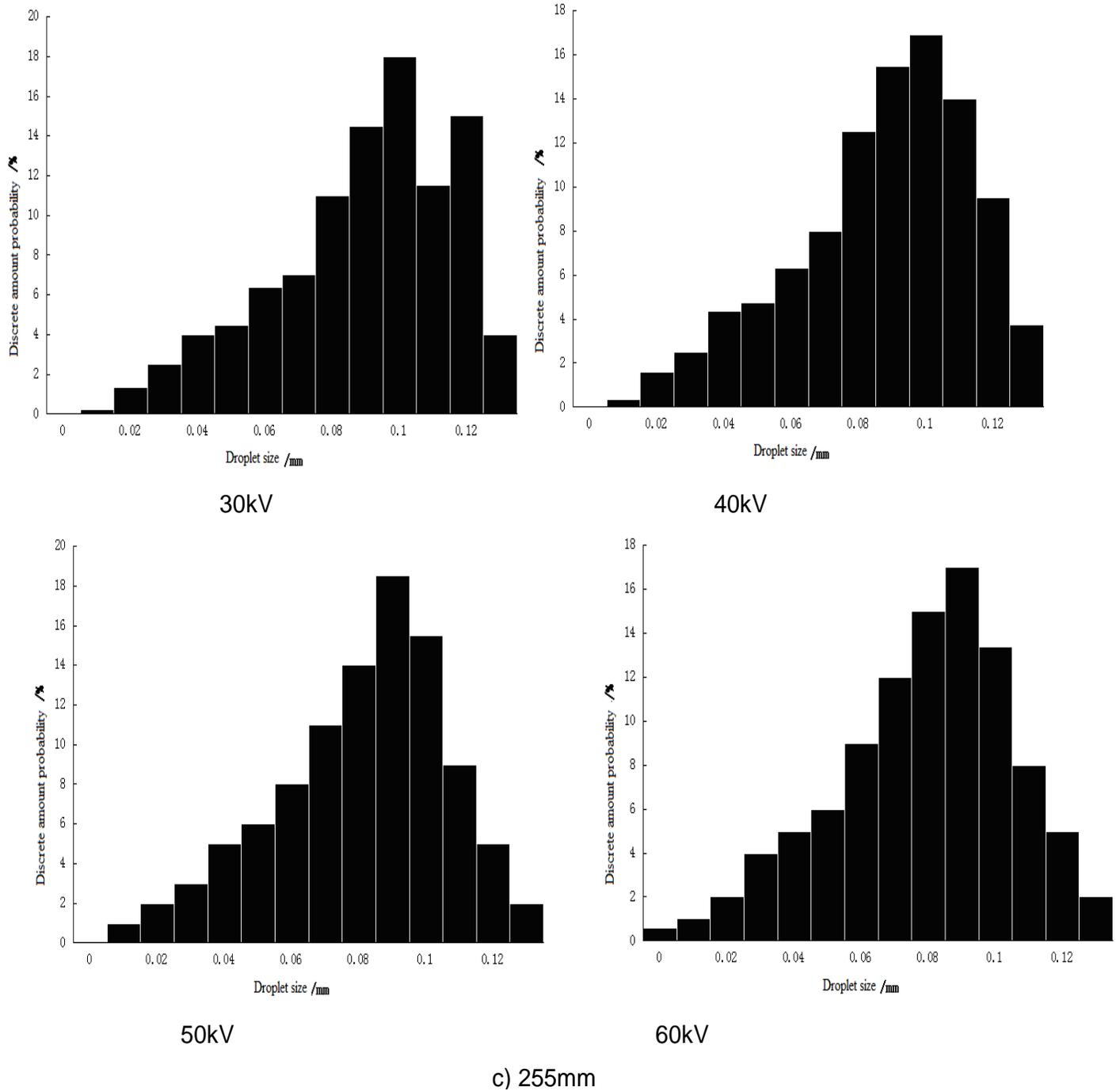
30kV
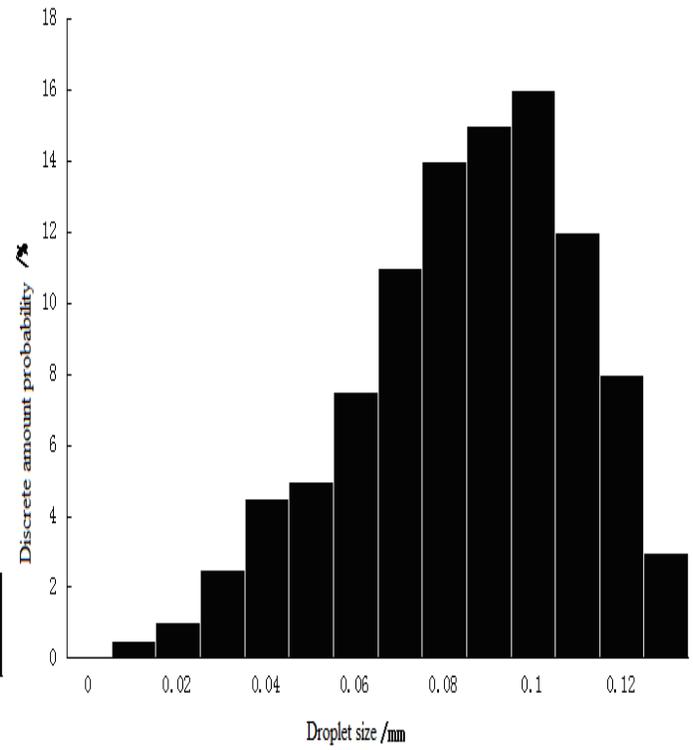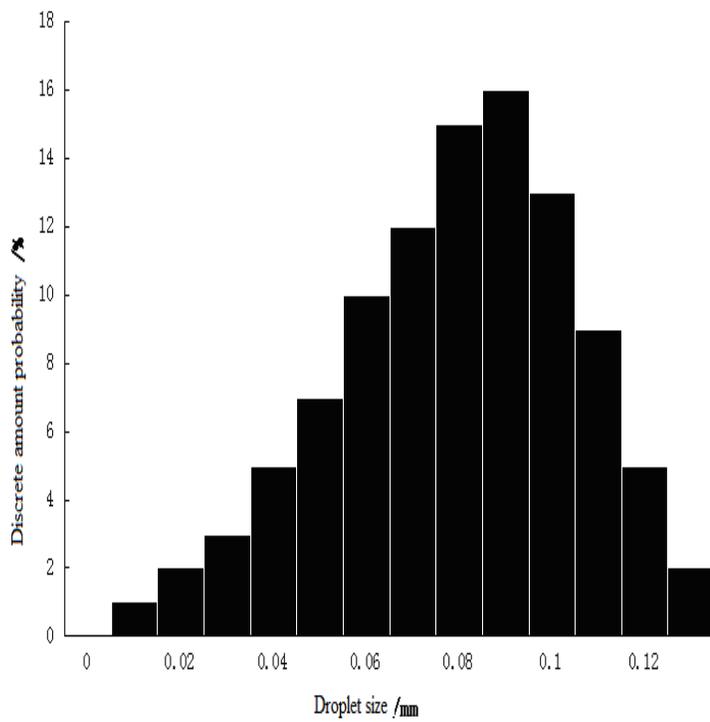
40kV

50kV

60kV

c) 255mm

Figure 12. Discrete probability distribution of droplet average diameter number under different operating voltages and electrode spacing.

metal plate. When the voltage between 30 and 40 kV, the droplet deposition density is lower at the center spraying axis. It gradually increased to reach the maximum amount in the deposition point coordinates of about 10 mm, and then the deposition density decreased rapidly along the radial direction. When the voltage rises to over 50 kV, the droplets' deposition amount is larger at the center axis and the deposition density is maximum. If the voltage is higher, the deposition density is greater. When the voltage is 70 kV, the droplet deposition amount is maximum at the center axis, then decreased along the radial direction gradually with the increasing voltage. It can be seen that when the voltage gets 50 to 60 kV and the electrode spacing is 195 to 225 mm, the droplet
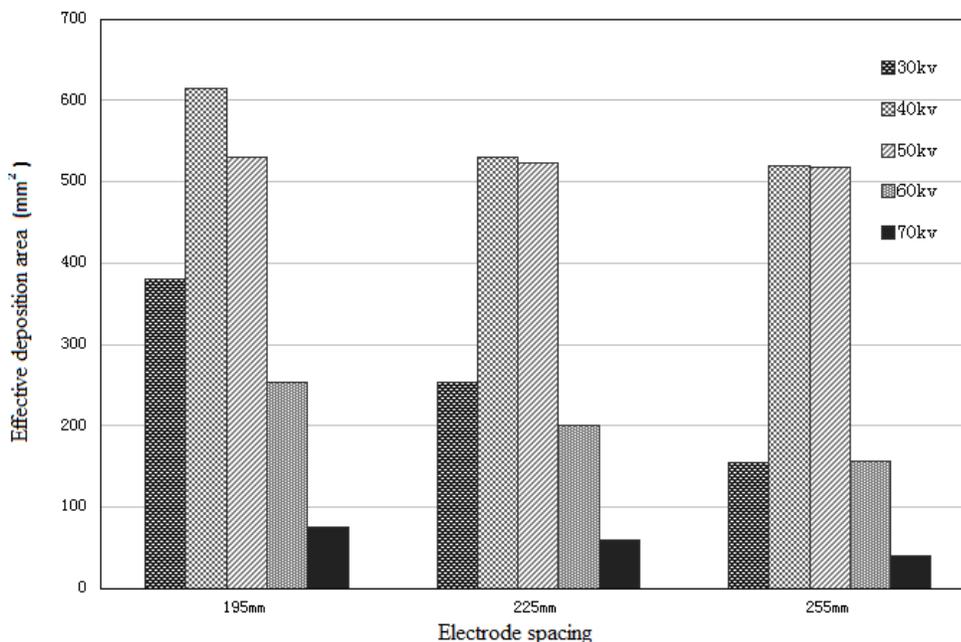
Figure 13. Droplet deposition area of different operating voltage and electrode spacing.

deposition density is the most uniform and the deposited amount is moderate. At that time, it indicates that the electrostatic spraying atomizing effect is better at this time.

EXPERIMENTAL

Experimental platform

The electrostatic spraying experimental is determined by two major distribution indexes: The spray droplet morphology and the particle size. We use SONY DSC-F717 speed camera to shoot the electrostatic atomizing fluid jet form at different voltage in spraying experiment. We use ATEST-212 type Spray Laser Particle Size Analyzer to measure the electrostatic spraying particle group scattering spectrum, and analyze the spray droplet size distribution by the computer data process. The electrostatic oiler room spraying experimental platform is shown in Figure 15.
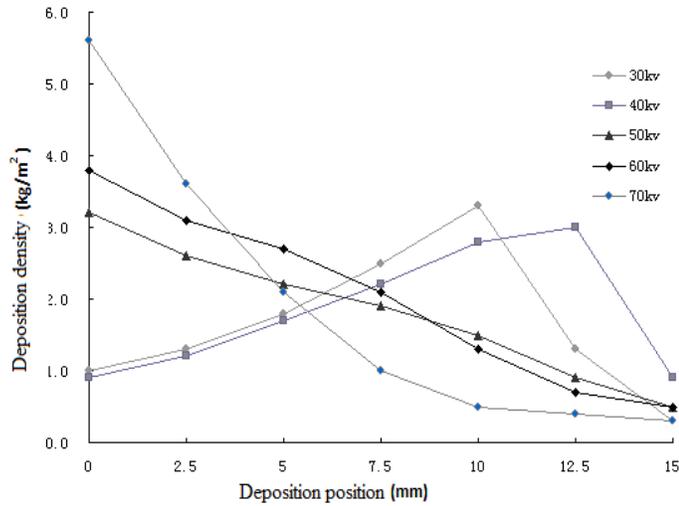
RESULTS AND DISCUSSION

Spray patterns

Figure 16 shows oil atomized form when the electrode spacing of 195 mm, and operating voltage at 30, 40, 50 and 60 kV. It can be seen that with the electrostatic oiler working voltage increasing, and the voltage between 30-50 kV, the droplet distribution is very uneven. At both sides of jet, the number of particles is more, and the number of intermediate particles is little. In the certain electrode spacing, the spray angle size directly determines the size of atomized droplets deposited area
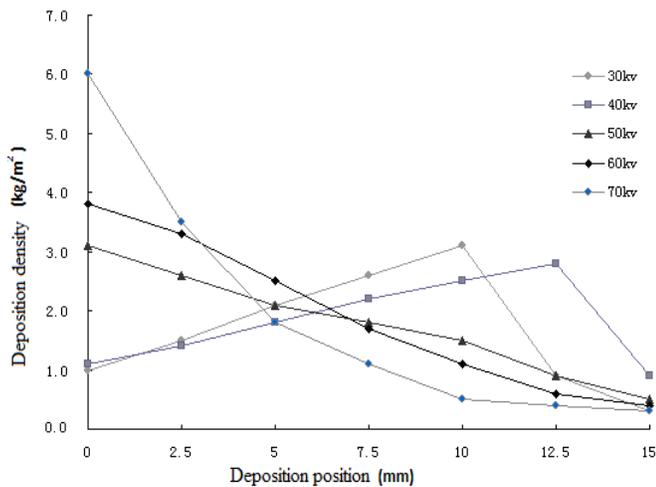
on the substrate surface, and it is identical with the trend of deposition area. When the working voltage is over 50 kV, the oil bifurcation disappears gradually, and the droplet distribution becomes uniform. When the voltage reaches 60 kV, the droplet distribution is uniform, the better atomization have achieved. The experimental data is basically consistent with the simulation results.
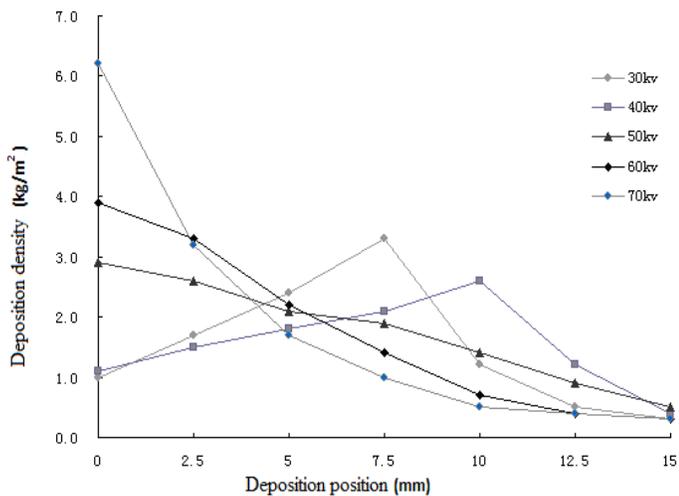
Spray particle size

The oil particle size distribution based on the analysis of Laser Particle Size analyzer Software is shown as Figure 17. When the voltage is 30 kV, the particle size distribution is bimodal shape; the range of the overall droplet particle size distribution is large. The range mainly is 90 to 120 µm. At this time due to the electrostatic voltage is low, the droplet atomization insufficient broken, and the overall particle size is large, the atomization is not satisfied. When the voltage rises to 50 to 60 kV, the particle size distribution exhibits a good normal distribution. The main distributed within the range of 80 to 100 µm, but oil particle size is relatively larger at this voltage. When the voltage increase to 60 kV, the range of particle size mainly in the 60 to 80 µm. The particle size continues to reduce and distributed more evenly at this time, and it is identical with the simulation of particle size distribution under the same electrode separation and voltage. Therefore, we believe the oil jet at around 60 kV, achieve a better atomization effect basically, and the electrostatic oiler operating voltage usually be selected at this voltage.

(a) 195 mm

Figure 15. Electrostatic spraying experimental platform.

(b) 225 mm

| 30 kV | 40 kV | 50 kV | 60 kV |

Figure 16. Electrostatic spraying pattern under different operating voltages.

(c) 255 mm

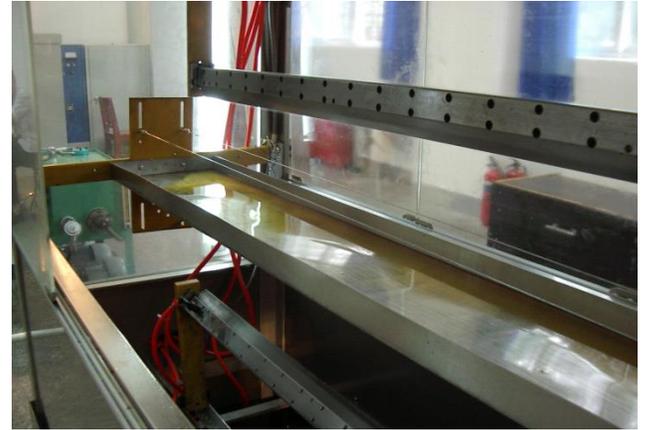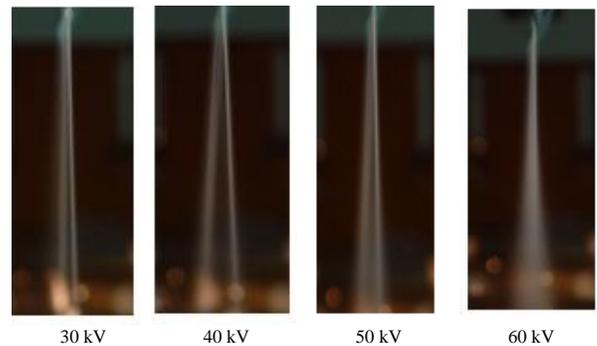**Figure 14.** Droplet deposition density distribution of different operating voltage and electrode spacing.

Conclusions

For electrostatic oiler, the droplet axial velocity is faster near the larger electric field strength. Near the central axis within a certain range, the droplet radial velocity has a maximum value. For electrostatic oiler, when the voltage keeps a certain value, the droplet deposition area decreases with the electrode spacing increasing. When the voltage increases from 30 to 40 kV, the deposition area increases obviously. When the voltage between 40 and 50 kV and the electrode spacing is 195 mm, the droplet deposition area achieves the maximum 615 mm^2. When voltage exceeds 60 kV, the droplet deposition area is dramatically reduced. When the voltage between 30 and 40 kV, at the center axis, the droplet deposition density is lower. Then it decreases rapidly after it achieves a certain value along the radial direction. When the voltage rises above 50 kV, at the center axis, the droplet deposition amount is larger, the deposition density is higher. What is more, the voltage being higher, the deposition density is greater. When the voltage between 50 and 60 kV and the electrode spacing between 195
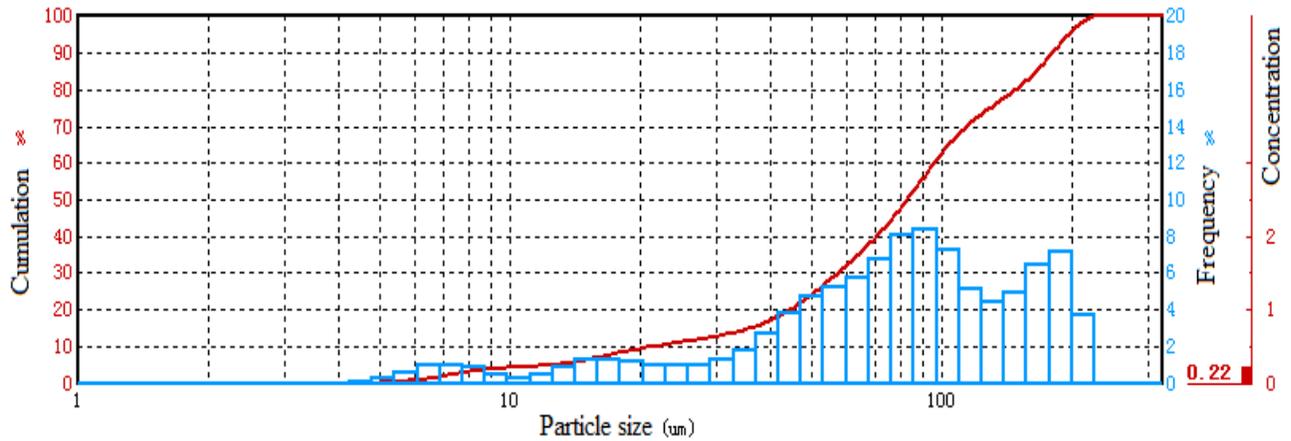
(a) 30 KV
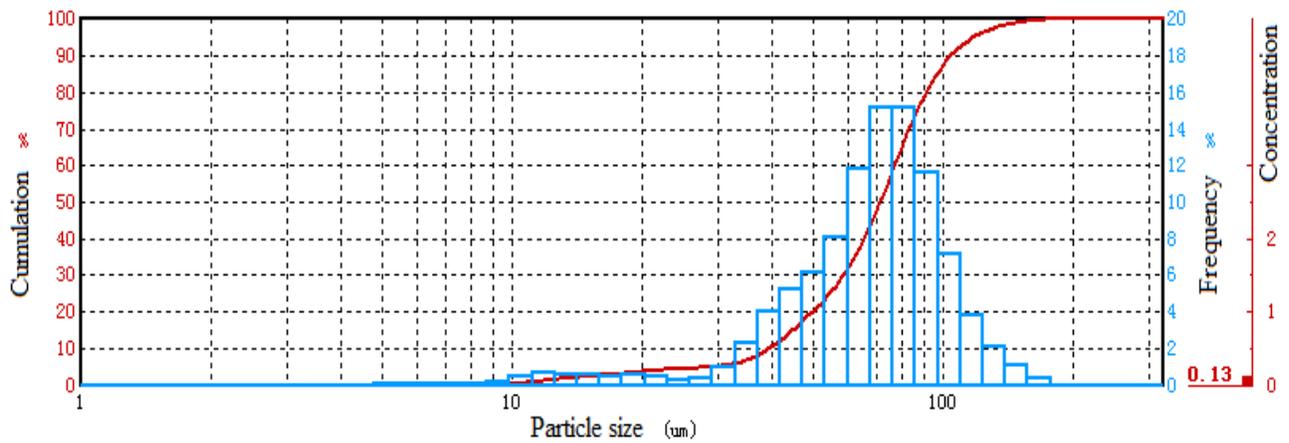
(b) 50KV
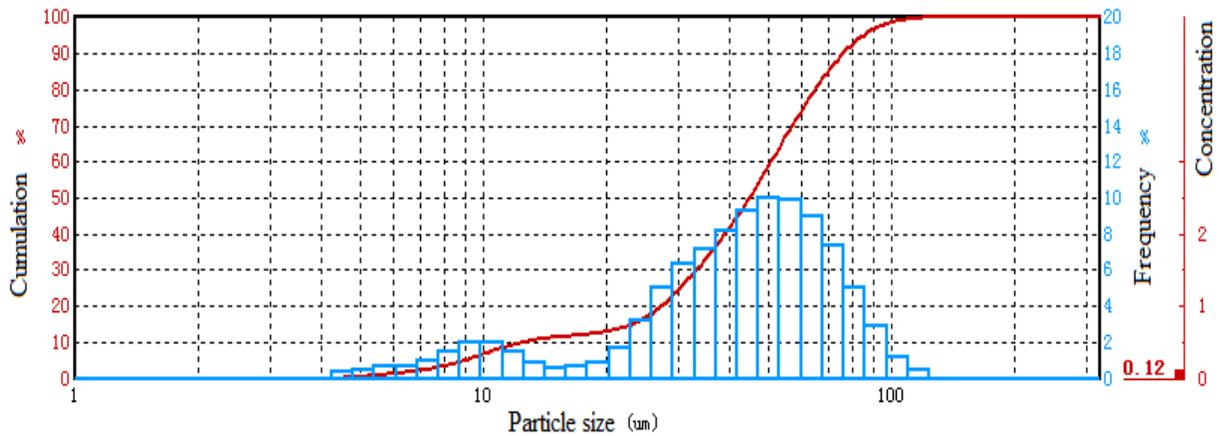
(c) 60 KV

Figure 17. Oil particle size distribution under different operating voltages.

and 225 mm, the droplet deposition density shows most uniform, and the deposition amount is moderate. At that time, the electrostatic spray atomization effect is better.

Conflict of Interests

The authors have not declared any conflict of interests.

ACKNOWLEDGMENT

REFERENCES

Chen HL, Zhao YC (2010). Electrostatic induction field and charging property of droplet in electrostatic spraying process. High Vohage Engineer. 36(10):2519-2524.

Colbert SA, Cairncross RA (2005). A computer simulation for predicting electrostatic spray coating patterns. Powder Technol. 151(1-3):77-86.

Doyle A, Moffett DR, Vonnegut B (1964). Behavior of evaporating electrically charged droplets. J. Colloid. Sci. 19(2):136-143.

Gu PD, Xu J, Liu YN (2010). Simulation of jet-cone model in electrostatic spray. J. Agric. Mechanization Res. 6:90-93.

Jung JH, Oh H, Sang SK (2010). Numerical simulation of the deposition pattern in multiple electrohydrodynamic spraying. Powder Technol. 198(3):439-444.

Ru Y, Jin L, Zhou HP, Jia Z (2014). Charging characteristics of droplets effect on the distribution and adhesion of droplets on target. (Natural Sciences Edition). J. Nanjing For. Univ. 38(3):129-133.

Sun GX, Wang XC, Ding WM, Zhang Y (2012). Simulation analysis on characteristics of droplet deposition base on CFD discrete phase model. Trans. Chin. Soc. Agric. Eng. 28(6):13-19.

Wang JF, Zhang JJ, Wang Z T, Huo Y, Wang Z (2012). Deposition and distribution characteristics of air-assisted electrostatic spraying by wind-curtain. Trans. Chin. Soc. Agric. Machinery 43(2):61-65.

Wang JF, Zuo ZW, Huo YP (2013). Numerical simulation of droplet and EHD cone jet formation process. J. Eng. Thermophys. 34(4):667-671.

Wang ZH, Gao QJ, Wang JQ, Huo Y, Wang Z (2011). Realization of atomizing animation for spraying based on OpenGL in the electrostatic oiler. Appl. Mech. Mater. 52-54:79-83.

Wang Z H, Jiang S W, Gao QJ (2013). Axisymmetric cone-jet model and numerical simulation for electrostatic spraying. Trans. Chin. Soc. Agric. Machinery 44(8):84-89.

Xie TQ, Yang QP, Jones BE, Butler C (2000). Optimization of air cone-jet sensor using 2D finite element analysis. Sensors Actuators Phys. 85(1):18-22.

Ye Q, Steigleder T, Scheibe A, Domnick J (2002). Numerical simulation of the electrostatic powder coating process with a corona spray gun. J. Electrostat. 54(2):189-205.

Zohdi TI (2013). Numerical simulation of the impact and deposition of charged particulate droplets. J. Comput. Phys. 233(233):509-526.